A major purpose of the Technical Information Center is to provide the broadest dissemination possible of information contained in DOE's Research and Development Reports to business, industry, the academic community, and federal, state and local governments.

Although a small portion of this report is not reproducible, it is being made available to expedite the availability of information on the research discussed herein.

LA-UR -83-3713

Los Alamos National Laboratory is operated by the University of California for the United States Department of Energy under contract W-7405-ENG-36

LA-UR--83-3713

DE84 004358

TITLE LINE WIDTH AND LINE SHAPE ANALYSIS IN THE INDUCTIVELY COUPLED PLASMA BY HIGH RESOLUTION FOURIER TRANSFORM SPECTROMETRY

AUTHOR(S) Lynda Margaret Faires, CHM-1
Byron Allen Palmer, CHM-1
James William Brault, National Solar Observatory

SUBMITTED TO 1984 Winter Plasma Conference on Spectrochemistry
San Diego, CA Jan 2-6, 1984

DISCLAIMER

Los Alamos Los Alamos National Laboratory
Los Alamos, New Mexico 87545

FORM NO. 836 R4
ST. NO. 2629 5/81

LINE WIDTH AND LINE SHAPE ANALYSIS IN THE INDUCTIVELY COUPLED PLASMA BY HIGH RESOLUTION FOURIER TRANSFORM SPECTROMETRY

Lynda M. Faires, Byron A. Palmer
Analytical Chemistry Group, Chemistry Division
Los Alamos National Laboratory
Los Alamos, New Mexico 78545

James W. Brault
National Solar Observatory
PO Box 26732
Tucson, Arizona 85726

ABSTRACT

High resolution Fourier transform spectrometry has been used to perform line width and line shape analysis of eighty-one iron I emission lines in the spectral range 290-390nm originating in the normal analytical zone of an inductively coupled plasma. Computer programs using non-linear least squares fitting techniques for line shape analysis were applied to the fully resolved spectra to determine Gaussian and Lorentzian components of the total observed line width. The effect of noise in the spectrum on the precision of the line fitting technique was assessed, and the importance of signal to noise ratio for line shape analysis is discussed. Translational (Doppler) temperatures were calculated from the Gaussian components of the line width and were found to be on the order of 6300K. The excitation temperature of iron I was also determined from the same spectral data by the spectroscopic "slope" method based on the Einstein-Boltzmann expression for spectral intensity and was found to be on the order of 4700K.

1. INTRODUCTION

Observed under even the highest of resolution, an atomic spectral emission line does not consist of a single frequency, but rather may be considered as an intensity versus frequency distribution with an intensity maximum at a central frequency ν_o and dropping off to zero intensity at some interval $\delta\nu$ on either side. The width of the spectal line is usually defined as the full width at half maximum of the intensity (FWHM) in units of frequency, wavelength, or wavenumber. There are several factors determining the width and broadening of spectral lines [1-5]:

(a) The natural line width is due to the finite lifetime of the atom in the excited state. The Heisenberg uncertainty principle relates the mean lifetime in the excited state to an uncertainty in the energy of the state and consequently a frequency distribution in the radiation emitted by the transition from that state. This natural line width is on the order of 10^{-5} nm in the UV-VIS and is generally negligible compared to other line broadening effects in analytical sources.

(b) The Doppler broadening is due to the random kinetic motion of the gas phase atoms relative to the point of observation during the emission process. A Maxwellian velocity distribution of the emitting atoms gives rise to line broadening which is Gaussian in shape and symmetric about the central frequency (Figure 1). The Doppler width of a spectral line $\Delta\nu_D$ can be expressed as

$$\Delta\nu_D = \left(\frac{2\nu_o}{c}\right)\left(\frac{2RT\ln 2}{M}\right)^{1/2} \qquad (1)$$

where ν_o is the spectral line center, R is the gas constant, T_D is the translational (or Doppler) temperature in degrees Kelvin, M is the atomic weight of the emitting species, and c is the speed of light. Conversely, if the Doppler width of a spectral line is known, the translational or Doppler temperature can be calculated from the relationship

$$T_D = \left(\frac{\Delta\nu_D}{\nu_o}\right)^2 \left(\frac{Mc^2}{8R\ln 2}\right) \qquad (2)$$

where

$$\left(\frac{\Delta\nu_D}{\nu_o}\right) = \left(\frac{\Delta\lambda_D}{\lambda_o}\right) = \left(\frac{\Delta\sigma_D}{\sigma_o}\right) \qquad (3)$$

and ν, λ, σ represent frequency, wavelength, and wavenumber units respectively.

(c) Pressure broadening is caused by collisions of the emitting species with other atoms in the gas phase. If collisions are with foreign atoms or molecules, it is called Lorentz broadening. If collisions are with like atoms it is called Holtzmark or resonance broadening. Lorentz broadening is usually the predominant case at concentration levels common to analytical

atomic spectroscopy and produces a Lorentzian shaped line profile (Fig. 1).

(d) Stark and Zeeman broadening occur if the excited atoms are subjected to strong electric or magnetic fields respectively.

(e) Self-absorption or self-reversal effects cause a decrease in intensity at the line center and a subsequent increase in the spectral line width measured at the full-width-half-maximum of the observed intensity.

(f) Hyperfine structure and isotope shifts produce apparently broadened lines due to the presence of separate but closely spaced and unresolved lines.

In a normal analytical source such as the inductively coupled plasma (ICP), line broadening will be primarily defined by contributions from the Doppler (Gaussian) and pressure (Lorentzian) effects. The observed spectral line profile will be a convolution of these Gaussian and Lorentzian components of the line shape and can be described by a Voigt profile [6] whose width is given by the empirical approximation

$$\Delta\nu_V = k\Delta\nu_L + (\Delta\nu_G^2 + (1-k)^2\Delta\nu_L^2)^{1/2} \qquad (4)$$

and where the constant term k equals .534. An a factor is often also defined to express the ratio of the Lorentzian width $\Delta\sigma_L$ to the Gaussian width $\Delta\sigma_G$ at FWHM:

$$a = \left(\frac{\Delta\sigma_L}{\Delta\sigma_G}\right)(\ln 2)^{1/2}. \qquad (5)$$

Spectral interferences in analytical atomic spectroscopy can be reduced by using a spectrometer of high dispersion and resolving power. However, the ultimate limiting factors are the inherent widths of the spectral lines. Further, knowledge of spectral line widths and line shapes (deconvolution into Gaussian and Lorentzian components of the observed total line profile) is useful for the characterization of spectraphysical properties and excitation mechanisms in the source. In spite of the popularity of the ICP as a source for analytical atomic emission spectrometry and the large number of studies published on spectraphysical properties of the source, relatively few studies have been made of line widths and shapes in the ICP because of the high resolution required for such measurements.

Human and Scott [7] used a Fabry-Perot interferometer to measure profiles of spectral lines of calcium, strontium, and argon. Larson and Fassel [8] discussed line broadening and radiative recombination interferences in the ICP. Broekaert, Leis, and Laqua [9] determined spectral line widths for eighteen lines of sixteen rare earth elements. Mermet and Trassy [10] discussed spectral line broadening in the ICP. Batal and Mermet [11] calculated line profiles in the ICP. And Kawaguchi et al. [12] measured line widths of fifteen spectral lines of ten elements in the ICP using a Fabry-Perot interferometer.

The purpose of this study was to determine line widths and line shapes of iron I lines in the normal analytical zone of the ICP using the high resolution capabilities of a Fourier transform spectrometer. The information is useful for evaluating spectral interferences for analytical applications and for elucidating spectraphysical characteristics of the ICP. The total observed line profiles can be deconvoluted by line fitting techniques into Gaussian (Doppler) and Lorentzian (pressure) components. Translational temperatures can be calculated from the Gaussian component of the total line width.

Excitation temperature in the source can also be determined by the "slope method" based on the Einstein-Boltzmann expression for spectral line intensity (13). Measuring the intensity in units of photons/sec by the Fourier transform technique reported here, the expression takes the form (14)

$$I_{nm}=\left(\frac{N_o}{g_o}\right)\left(\frac{8\pi^2e^2}{mc}\right)\left(\frac{g_m f_{mn}}{\lambda^2_{nm}}\right)(\exp -E_n/kT). \qquad (6)$$

where N_o is the number of atoms in the ground state, g_o is the statistical weight of the ground state, g_m is the statistical weight of the lower state m, f_{mn} is the oscillator strength of the transition from state m to n, λ_{nm} is the wavelength of the transition, E_n is the energy of the upper state n, k is the

Boltzmann constant, and T is the excitation temperature. By measuring the

relative intensities of a number of transitions of the same thermometric species and plotting

$$\ln\left(\frac{I_{nm}\lambda^2_{nm}}{g_m f_{mn}}\right) \text{ versus } (E_n) \qquad (7)$$

a "Boltzmann plot" is obtained with a slope equal to $(-1/kT)$ where T is the desired excitation temperature for that thermometric species in the source.

2. EXPERIMENTAL

2.1. INSTRUMENTATION

The ICP emission spectrum of iron I was recorded on the high resolution Fourier transform spectrometer located in the McMath Solar Telescope at Kitt Peak National Observatory [15]. General characteristics of this instrument and details pertinent to this study are summarized in Table 1. A Plasma Therm 2500 series ICP torch box was secured 118 cm in front of the Fourier transform spectrometer, and the plasma image was focused onto the spectrometer aperture and magnified by a factor of 4.5 by a single quartz lens. Operating parameters for the ICP were set to simulate normal analytical conditions and are summarized in Table 2. The viewing zone was selected at 11 mm above the top induction coil (as illustrated in Figure 2) in the normal analytical zone [16], the plasma region used for most analytical measurements. A high efficiency fritted-disc nebulizer developed in this

laboratory [17,18] was used because the fine, homogeneous aerosol produced in this nebulizer was expected to reduce noise in the source due to very short time scale (msec or less) spikes and variations of emission intensity in the plasma which result from the vaporization and excitation of analyte in non-uniform aerosol droplet distribution. This nebulizer design is shown schematically in Figure 3.

2.2 METHOD

The spectrum of a 1000 µg/ml solution of iron metal in .1 molar HNO_3 was recorded over the spectral range 290-390 nm. Filters were used at the detector to limit the spectral region being observed to a narrow range in order to improve the quality of the signal to noise ratio in the spectrum. A maximum optical path difference in the interferometer of 7.06 cm resulted in a resolution of 0.071 cm^{-1} (.00086 nm at 350 nm). Twenty-four scans of the 10^6 point interferogram were co-added to further improve the signal to noise ratio in the resulting spectrum. Relative intensities (determined as peak heights) were corrected for instrumental response using a calibrated quartz iodine lamp. Spectral line identification was based on NBS [19] wavelength tables.

2.3 DATA ANALYSIS

The analysis of the spectrum was based on the assumption that the only significant contributions to the observed line widths were due to Doppler and Lorentzian broadening. Some microturbulent broadening may also be expected, but it would be

indistinquishable from the thermal Doppler broadening, and its effect would be to increase the Gaussian component to the line width. Thus, the appropriate model for the line shape is the Voigt function. for computational convenience, the formulation by Elste [20] was used. In this representation, the four parameters which specify the profile are: central wavelength or wavenumber, the full width at half maximum of intensity (FWHM), the peak intensity, and a shape parameter $b_1 = (1/2)(\Delta\sigma_L/\Delta\sigma)$.

Since some of these parameters enter into the analysis in a non-linear way, the problem was linearized as usual by choosing approximate starting values for the parameters and treating the residuals (observed minus calculated) as a linear combination of the derivatives of the Voigt function with respect to the parameter values. The coefficients of these derivatives are then adjusted to minimize the residual; the final coefficients are the corrections to the original starting values. This process is repeated until values converge, usually in 2-4 iterations.

The Lorentzian component of the line width follows immediately from the FWHM and the shape parameter. The Gaussian component of the line width was found from Eqn. (4). In general, this representation of the spectral lines was completely satisfactory after a small background contribution had been subtracted.

3. RESULTS AND DISCUSSION

A representative section of the iron spectrum used in this study is illustrated in Figure 4. This plot of two iron I lines at 297.323 nm and 297.313 shows the quality of resolution in the recorded spectrum; these two lines differ by 0.01 nm and are clearly separated by baseline resolution. The line shapes shown here are the actual profiles of the spectral lines. The resolving power capability of the Kitt Peak Fourier transform spectrometer eliminates the necessity of further corrections for instrumental effects.

3.1 EFFECTS OF NOISE ON LINE SHAPE ANALYSIS

The criteria for good line shape analysis include: resolution adequate to make instrumental corrections negligible compared to the noise; absence of spectral interferences, blends, and hyperfine structure in the chosen lines; and good signal to noise characteristics in the spectrum. Figure 5 repeats the plot of the two iron I lines illustrated in Figure 4, but in this case the intensity axis has been magnified eight times to reveal the complexity of the signal near the baseline where the spectral line is comparable to the noise present in the spectrum. This makes exact fitting of the observed line shape impossible, and some degree of error is introduced into the line shape analysis depending on the signal to noise ratio of the lines being considered.

In order to assess the magnitude of this error, a set of "test" data was created by selecting a portion of the baseline of the observed iron spectrum where no emission lines were present

but where the noise was typical of that present throughout the spectrum. A set of 50 artificial lines of predefined total width, predefined Gaussian and Lorentzian composition, and three different intensity (signal to noise) levels were superimposed on the real noise of the spectral baseline. This synthetic spectrum was then analyzed by the same techniques as have been applied to the experimental spectrum. Some results of this test are summarized in Tables 3 and 4.

The test data clearly emphasize the importance of good signal to noise characteristics for good line width and line shape analysis. The precisions (expressed as percent relative standard deviations of the means) of the line intensity and the total observed line width $\Delta\sigma$ are similar and are directly proportional to the signal to noise ratio of the lines so that as the signal to noise ratio increases by an order of magnitude so does the precision of the intensity and line width determinations. The precision of the determination of the Gaussian component of the total observed line width $\Delta\sigma_G$ is related to the signal to noise ratio by the same direct proportionality, but is less precise than the total line width by a factor of approximately three in the test data. The precision of the determination of the Lorentzian component of the total line width $\Delta\sigma_L$ is also proportional to the signal to noise ratio, but is less precise than the total line width by a factor of approximately thirty in the test data. These exact factors are a result of the choice of the degree of Gaussian and Lorentzian composition in the total line width that was

selected for the synthetic lines in the test data to approximate the character of the observed lines in the experimental data. Had the Lorentzian component been chosen to represent a larger contribution to the total line width, the direct proportionality of precision to signal to noise ratio would have been maintained, but the precision of the determination would have been improved.

For a given translational (Doppler) temperature T_D in the source and a given thermometric species, the factor $\Delta\sigma_G/\sigma$ (Gaussian component in kaysers/wavenumber) should be constant, according to rearrangement of Eqn. (2):

$$\Delta\sigma_G/\sigma = (7.16X10^{-7})\ (T/M)^{1/2}. \qquad (8)$$

Table 4 summarizes the relationship between signal to noise and precision of $\Delta\sigma_G$ and translational temperature T_D calculated from $\Delta\sigma_G/\sigma$ for the test data. Figure 6 illustrates the variation of $\Delta\sigma_G/\sigma$ for the 199 iron I lines identified in the experimental spectrum. It is clearly shown here that a high degree of error in $\Delta\sigma_G$ occurs for those lines with low signal to noise ratio, and that this error is greatly reduced for those lines with higher signal to noise ratio.

For these reasons, only those iron I lines in the experimental spectrum with a signal to noise ratio greater than 100 were selected for the line shape analysis results reported here.

3.2 LINE SHAPE ANALYSIS AND TRANSLATIONAL TEMPERATURE

Table 5 summarizes the results of the line width and line shape analysis for the eighty-one iron I lines with signal to noise ratio greater than 100 in the observed spectral range. Tabulated for each line are: wavenumber in kaysers (cm^{-1}), wavelength in nanometers (nm), signal to noise ratio in the experimental spectrum, total observed line width in nanometers ($\Delta\lambda$), total observed line width in kaysers ($\Delta\sigma$), Gaussian component in kaysers ($\Delta\sigma_G$), Lorentzian component in kaysers ($\Delta\sigma_L$), the Voigt profile a factor, Gaussian component in kaysers divided by the wavenumber ($\Delta\sigma_G/\sigma$), and translational temperature (T_D) calculated from the Gaussian component for that transition. The Gaussian and Lorentzian components given in the table can be easily translated from units of kaysers to nanometers by the simple equation

$$\Delta\lambda = \lambda\ (\Delta\sigma/\sigma). \tag{9}$$

The translational (Doppler) temperature T_D was calculated from the Gaussian component of each transition. The mean value of T_D from all 81 iron I lines was 6310K with a relative standard deviation of 3.44% (217K).

3.3 IRON I EXCITATION TEMPERATURE

Excitation temperatures were determined for iron I using the spectroscopic "slope" method based on the Einstein-Boltzmann expression for spectral line intensity. This method has been

combined with Fourier transform spectrometry and applied to a study of the excitation temperature vertical profile for iron I in the inductively coupled plasma [14], and the critical importance of the choice of reference values for oscillator strength (gf) values for this method of temperature determination has been demonstrated [14,21]. The oscillator strength values for iron I used in this study were taken from BLACKWELL et al. [22-28], BRIDGES and KORNBLITH [29], and HUBER and PARKINSON [30]. A recent compilation or transition probabilities for iron I [31] considers the values from BLACKWELL et al. to be quite good and those from BRIDGES and KORNBLITH to be fairly accurate. The results of the excitation temperatures determined in this manner are summarized in Table 6. Again, only those lines with signal to noise ratio greater than 100 were used. The three different values of the excitation temperature derived from each of the three different references selected for the gf values are all in agreement within the estimated error of each value and are all on the order of 4700K. This value is somewhat lower than previous values determined in a similar manner [14] under similar conditions. The main difference in the two experimental arrangements was a change from a concentric nebulizer used in the earlier study to the fritted-disc nebulizer used in this study. Differences in the flow dynamics of the two nebulizers make it reasonable to expect some effect on the plasma temperature. The Boltzmann plot for the excitation temperature determination using the iron I gf values from BLACKWELL et al. is illustrated in

Figure 7. This plot is seen to be quite linear, and the resulting uncertainty in the temperature calculated from the slope of this plot is about one percent. An outstanding advantage of applying Fourier transform spectrometry techniques to spectraphysical studies of this type is also illustrated here. The powerful information gathering ability of a Fourier transform spectrometer allows the simultaneous and accurate recording of all the emission lines within the selected bandpass so that the Boltzmann plot can be constructed from the relative intensities of a large number (here 31-61) of spectral lines, thus improving the statistical precision of the resulting temperature.

4. CONCLUSIONS

A high resolution Fourier transform spectrometer has been used to record the spectrum of iron in the normal analytical zone of the inductively coupled plasma in the spectral range 290-390 nm. Non-linear least squares computer fitting techniques have been applied to the fully resolved spectra to determine the Gaussian and Lorentzian components of the total observed line profiles for 81 iron I lines with signal to noise ratio greater than 100 in the experimental spectrum. The total observed line widths for the iron I lines in this spectral range were found to be on the order of .003 nm. The Gaussian component was determined to be the dominant contribution to the total line shape, but the Lorentzian component does also contribute significantly. The Voigt a factors calculated from the ratios of Lorentzian to Gaussian components were on the order of 0.10. Translational

temperatures calculated from the Gaussian components for the 81 iron I lines resulted in a mean value of 6310K with a relative standard deviation of 3.44% (217K). Excitation temperatures for iron I determined by the "slope method" based on the Einstein-Boltzmann expression for spectral line intensity and using three different sets of reference values for iron I oscillator strengths were found to be on the order of 4700K with relative standard deviation of approximately 1.3% (62K).

The significant difference in the translational temperature and the excitation temperature derived from the same set of experimental data in this study is greater than the estimated error in each determination and implies some interesting physics in the source which are yet to be explained. A common conclusion from such diverse temperature values in a source is the absence of thermodynamic equiblibrium, as has already been proposed in the case of the ICP. However, the linearity of the Boltzmann plot in Figure 7 implies that the deviation from thermodynamic equilibrium in the source in this experiment would not be expected to be great enough to account for the rather large difference in the two types of temperatures measured here. It is postulated here that some other physical explanation is required, that the excitation temperature reported here is probably the better indication of the energy characteristics of the source, and that there may be other mechanisms in the source which contribute to the Gaussian component of the line profile causing it to appear broader than would be expected from the Doppler effect alone. Certainly there

is interesting research still to be pursued in explaining the spectrophysical properties of the ICP.

ACKNOWLEDGEMENTS

This work was performed under the auspices of the United States Department of Energy and the National Science Foundation at Los Alamos National Laboratory, Los Alamos, New Mexico, and at Kitt Peak National Observatory, Tucson, Arizona.

REFERENCES

[1] R.D. Cowan, Theory of Atomic Structure and Spectra, Univ. Calif. Press, Berkeley (1981).

[2] R. Mavrodineau, H. Boiteux, Flame Spectroscopy, Wiley, New York (1965).

[3] A.P. Thorne, Spectrophysics, Chapman and Hall, London (1974).

[4] H.G. Kuhn, Atomic Spectra, Academic Press, New York (1962).

[5] W.G. Shrenk, Analytical Atomic Spectroscopy, Plenum Press, New York (1975).

[6] D.W. Posener, Australian J. Phys. 12, 184 (1959).

[7] H.G.C. Human, R.H. Scott, Spectrochim. Acta 31B, 459 (1976).

[8] G.F. Larson, V.A. Fassel, Appl. Spect. 33, 592 (1979).

[9] J.A.C. Broekaert, F. Leis, K. Laqua, Spectrochim. Acta 34B, 73 (1979).

[10] J.M. Mermet, C. Trassy, Spectrochim. Acta 36B, 269 (1981).

[11] A. Betal, J.M. Mermet, Spectrochim. Acta 36B, 993 (1981).

[12] H. Kawaguchi, Y. Oshio, A. Mizuike, Spectrochim. Acta 37B, 809 (1982).

[13] I. Relf, V.A. Fasse R.N. Kniseley, Spectrochim. Acta 28B, 105 (1973).

[14] L.M. Faires, B.A. Palmer, R. Engleman, Jr., T.M. Niemczyk, submitted to Spectrochim. Acta (1983).

[15] J.W. Brault, Osserv. e Mem. dell Osserv. Astr. di Arcetri 106, 33 (1979).

[16] S.R. Koirtyohann, J.S. Jones, D.A. Yates, Anal. Chem. 52, 1965 (1980).

[17] C.T. Apel, D.V. Duchane, Pittsburgh Conf. on Anal. Chem. and Appl. Spect., Conf. Paper No. 411 (1979).

[18] D.L. Gallimore, C.T. Apel, Pittsburgh Conf. on Anal. Chem. and Appl. Spect., Conf. Paper No 398 (1981).

[19] C.H. Corliss, J.L. Tech, Oscillator Strengths and Transition Probabilities for 3288 Lines of Fe I, National Bureau of Standards Monograph 108, United States Department of Commerce, Washington, D.C. (1968).

[20] G. Elste, Z. Astrophys. 33, 39 (1953).

[21] I. Reif, V.A. Fassel, R.N. Kniseley, Spectrochim. Acta 31B, 377 (1976).

[22] D.E. Blackwell, B.S. Collinge, Mon. Not. R. Astr. Soc. 157, 255 (1972).

[23] D.E. Blackwell, P.A. Ibbetson, A.D. Petford, ibid. 171, 195 (1975).

[24] D.E. Blackwell, P.A. Ibbetson, A.D. Petford, ibid. 177, 219 (1976).

[25] D.E. Blackwell, P.A. Ibbetson, A.D. Petford, M.J. Shallis, ibid. 186, 633 (1979).

[26] D.E. Blackwell, A.D. Petford, M.J. Shallis, ibid. 186, 657 (1979).

[27] D.E. Blackwell, M.J. Shallis, ibid. 186, 669 (1979).

[28] D.E. Blackwell, A.D. Petford, M.J. Shallis, G.J. Simmons, ibid. 191, 445 (1980).

[29] J.M. Bridges, R.L. Kornblith, Astrophys. J. 192, 793 (1974).

[30] M.C.E. Huber, W.H. Parkinson, Astrophys. J. 172, 229 (1972).

[31] J.R. Fuhr, G.A. Martin, W.L. Weise, S.M. Younger, J. Phys. Chem. Ref. Data 10(2), 305 (1981).

FIGURE CAPTIONS

Figure 1. The line profiles for Gaussian (solid) and Lorentzian (dashed) line shapes having equal peak intensity and equal FWHM.

Figure 2. Schematic view of the ICP. The small circle represents the region of the plasma in the normal analytical zone selected for spectroscopic observation.

Figure 3. Schematic diagrams of the Los Alamos fritted-disc nebulizer design. Top figure shows end view. Sample is peristaltically pumped through the sample inlet capillary tube and deposited on the front surface of the fritted-disc. Argon carrier flow through the gas inlet tube produces fine aerosol which is swept out of nebulizer and into torch through the aerosol outlet (side view, bottom figure).

Figure 4. Actual quality of resolution in the FTS spectrum. Two iron I lines with wavelength separation of .01 nm are baseline resolved. The line profiles seen here are the fully resolved line shapes; no corrections are required for instrumental effects.

Figure 5. The iron I line profiles from Figure 4 shown at 8X magnification of the intensity axis. The effect of noise in the spectrum on the shape of the line profiles near the baseline which introduces error into the line shape analysis is illustrated.

Figure 6. Plot of $(\Delta\sigma_G/\sigma)$ X 10^5 versus signal to noise ratio for the 199 iron I lines observed in the experimental spectrum. The quantity $(\Delta\sigma_G/\sigma)$ should be constant for a given translation temperature in a source and a given element. The large scatter in the points with low signal to noise ratio indicate the inadvisability of using lines with low signal to noise ratio to calculate translational temperatures in a source.

Figure 7. Boltzmann plot of $(I\lambda^2/gf)$ versus E_{upper} for the determination of excitation temperature using 51 iron I lines in the experimental spectrum with signal to noise ratio greater than 100 and using gf values from BLACKWELL [22-28]. The excitation temperature determined from the slope (-1/kT) of the plot was 4732K with an estimated error of 62K.

Table 1. The Kitt Peak Fourier transform spectrometer: general characteristics and capabilities of the instrument as well as the capabilities utilized in this experiment are listed.

Table 2. ICP operating conditions: the operating parameters were adjusted to simulate normal analytical working conditions in the source.

Table 3. Test data showing the relationship between signal to noise ratio in the spectrum and the precision (expressed as percent relative standard deviation of the mean) of the determination of intensity (INT), total line width ($\delta\sigma$), Gaussian component of the line width ($\delta\sigma_G$), and Lorentzian component of the line width ($\delta\sigma_L$) for three sets of artificial lines with predefined characteristics superimposed on the noise of the experimental spectrum.

Table 4. Test data showing the relationship between signal to noise ratio in the spectrum and the precision (expressed as percent relative standard deviation of the mean) of the determination of the Gaussian component of the line width ($\Delta\sigma_G$) and the translational temperature T_D calculated from $\Delta\sigma_G$. Special note should be made of the inadvisability of calculating translational temperatures from lines with low signal to noise ratio.

Table 5. Results of the line shape analysis for 81 iron I lines with signal to noise ratio greater than 100 in the experimental spectrum. Results tabulated here include: wavenumber in cm^{-1} (σ), wavelength in nm (λ), signal to noise in the spectrum (S/N), total observed line width in wavenumbers ($\Delta\sigma$), total observed line width in nm ($\Delta\lambda$), Gaussian component of the line width in wavenumbers ($\delta\sigma_G$), Lorentzian component of the line width in wavenumbers ($\Delta\sigma_L$), Voigt a factor, Gaussian component in wavenumbers divided by wavenumber ($\overline{\Delta}\sigma_G/\sigma$), and translation temperature (T_D) calculated from the Gaussian component.

Table 6. Iron I excitation temperatures determined by the spectroscopic "slope method." Boltzmann plots were constructed using three different sets of gf values: BLACKWELL et al. [22-28], BRIDGES and KORNBLITH [29], and HUBER and PARKINSON [30]. The number of lines used to construct each Boltzmann plot indicated the number of lines in the experimental spectrum with signal to noise ratio greater than 100 for which gf values were also available in each of the references.

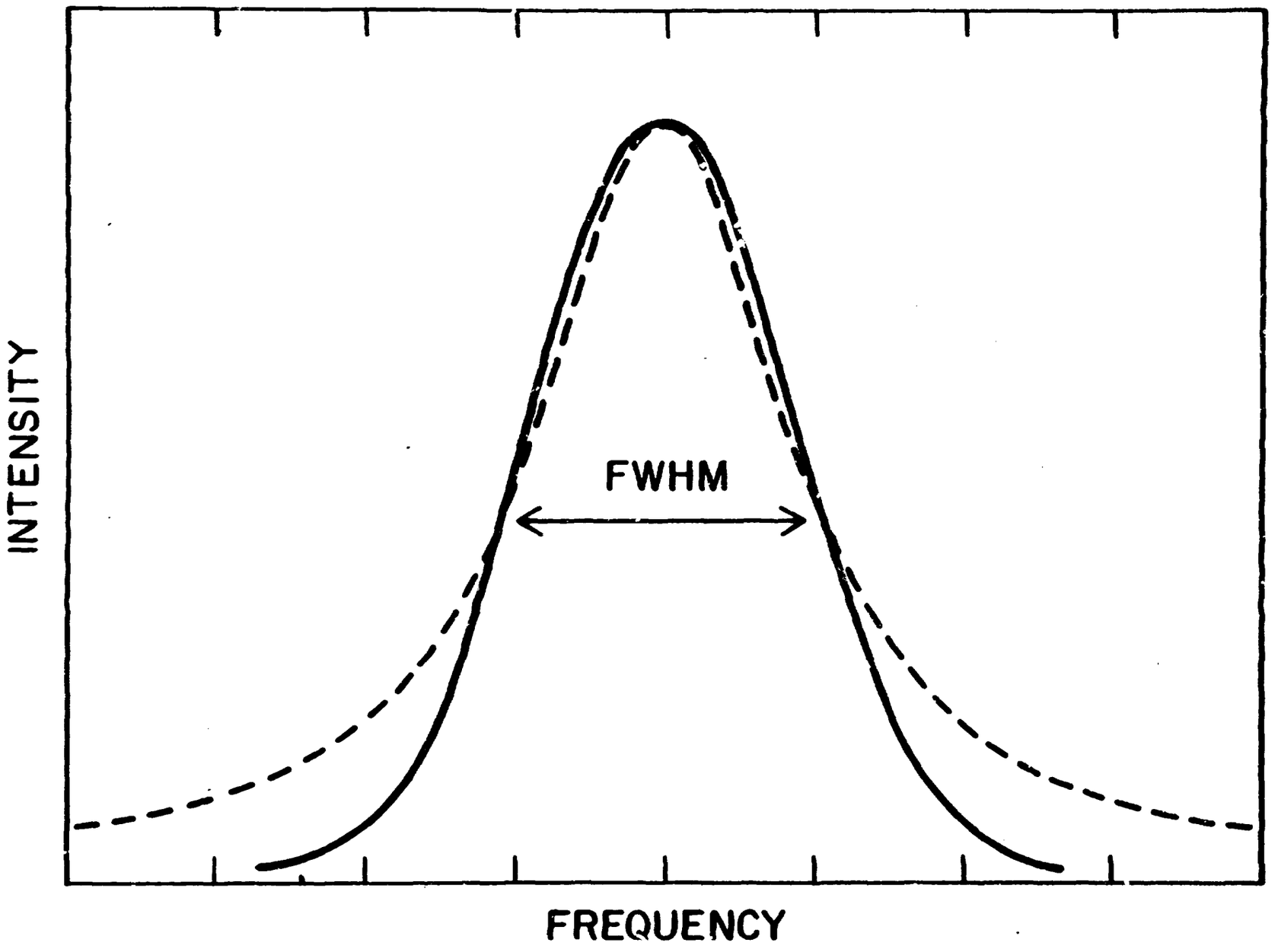

Figure

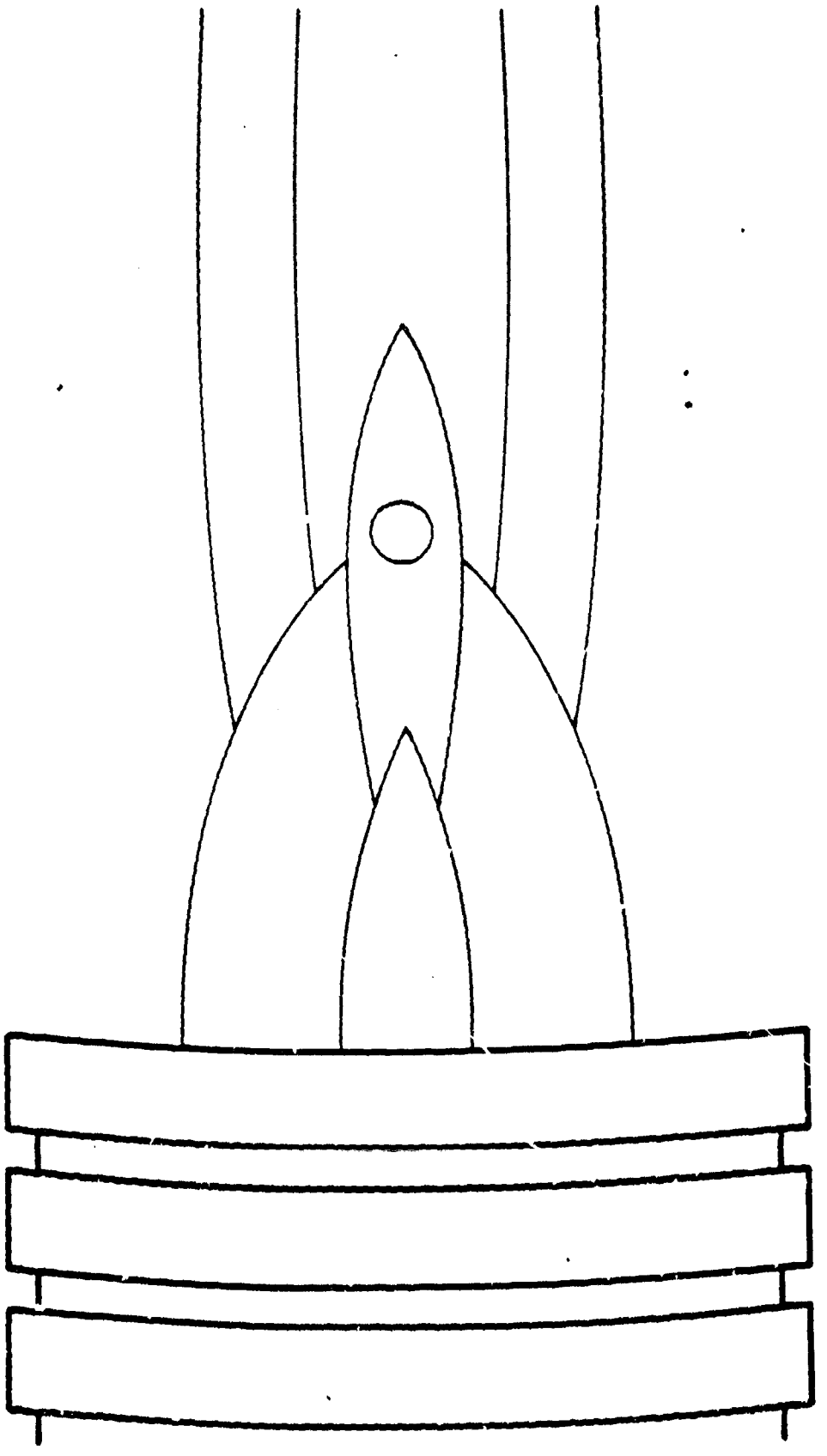

Figure

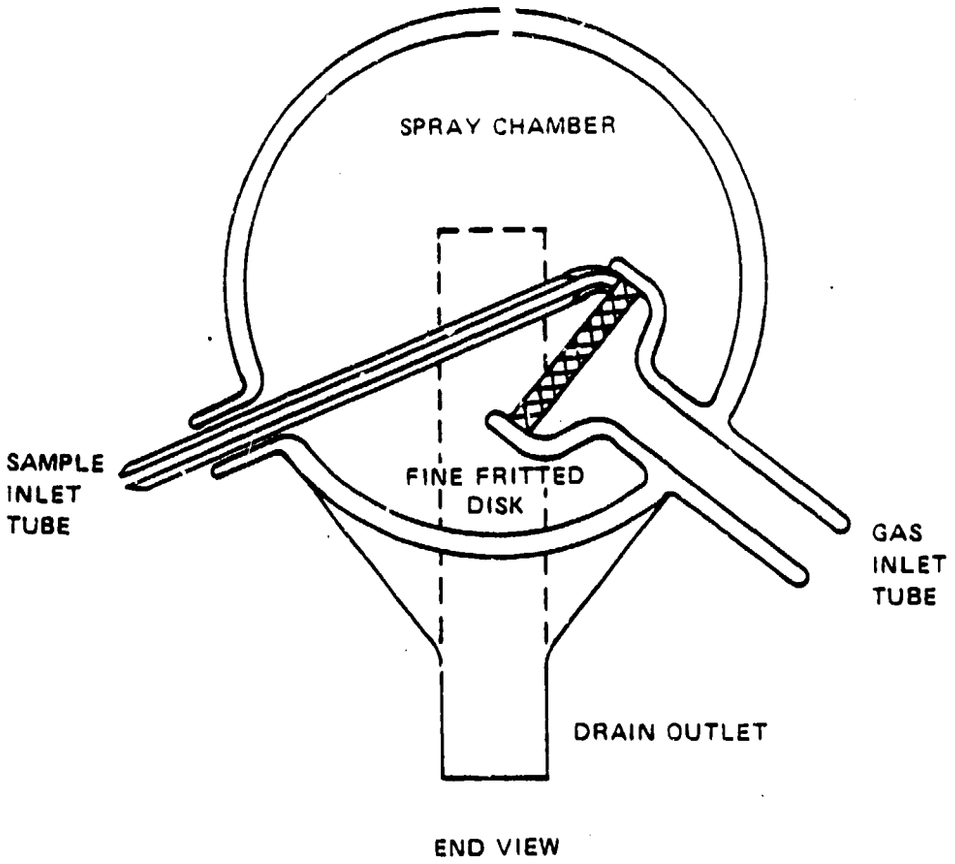
SPRAY CHAMBER
SAMPLE
INLET
TUBE
FINE FRITTED
DISK
GAS
INLET
TUBE
DRAIN OUTLET
END VIEW

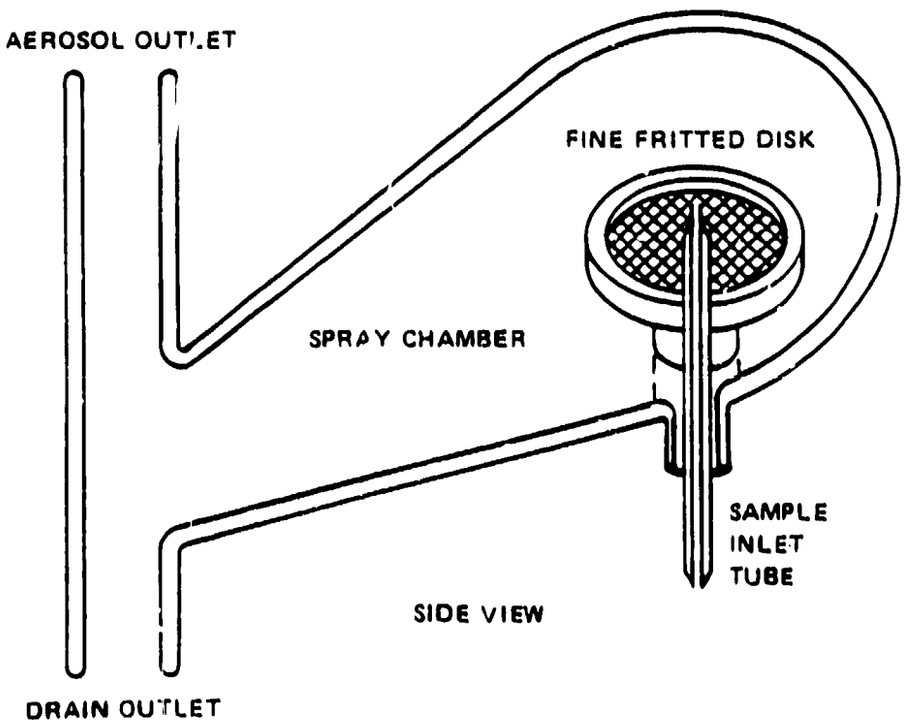
AEROSOL OUTLET
FINE FRITTED DISK
SPRAY CHAMBER
SAMPLE
INLET
TUBE
SIDE VIEW
DRAIN OUTLET

Figure 3

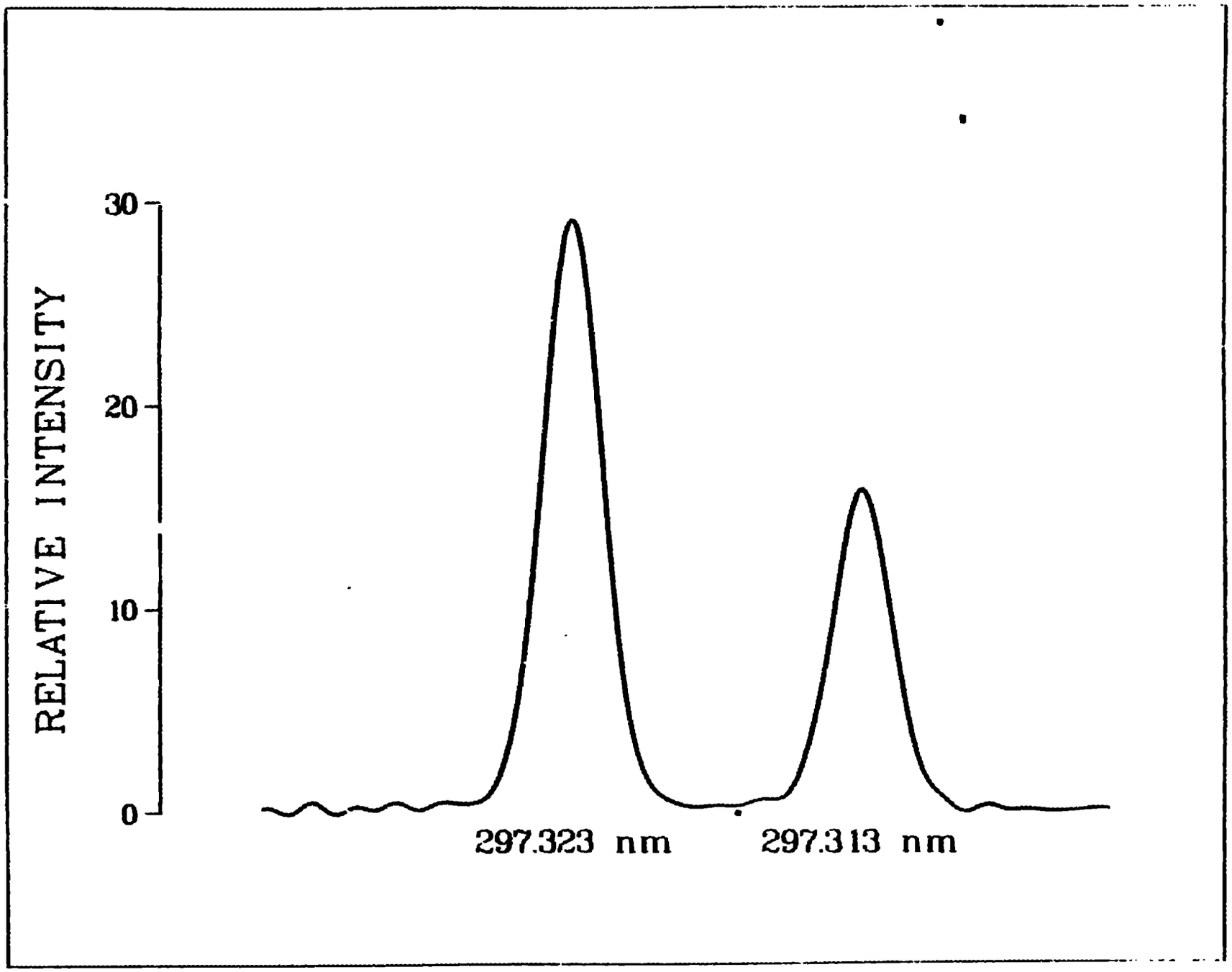

Figure 4

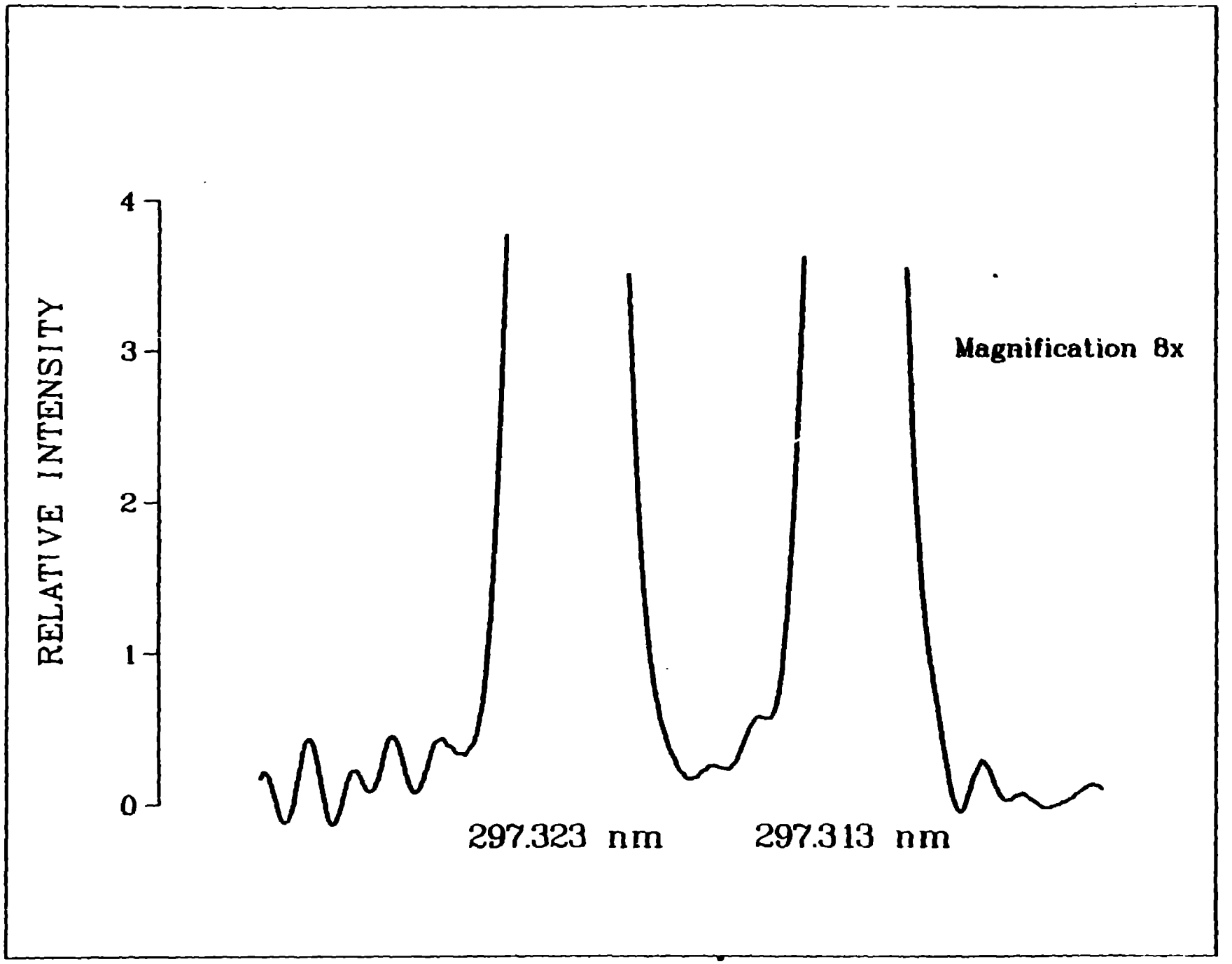
RELATIVE INTENSITY
4
3
2
1
0
Magnification 8x
297.323 nm
297.313 nm

Figure 5

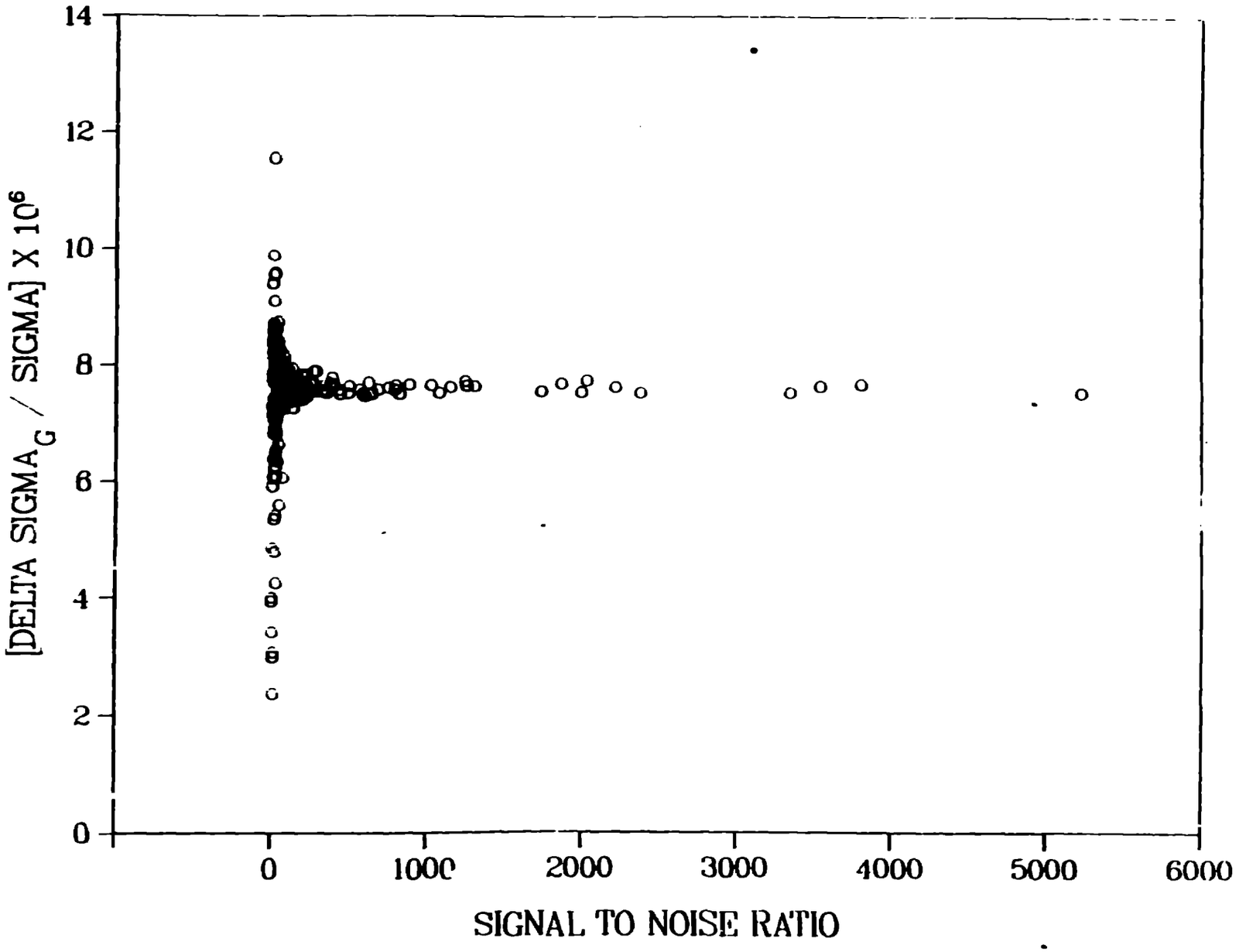
14
12
10
8
6
4
2
0
[DELTA SIGMA$_G$ / SIGMA] X 10^6
0
1000
2000
3000
4000
5000
6000
SIGNAL TO NOISE RATIO

Figure 6.

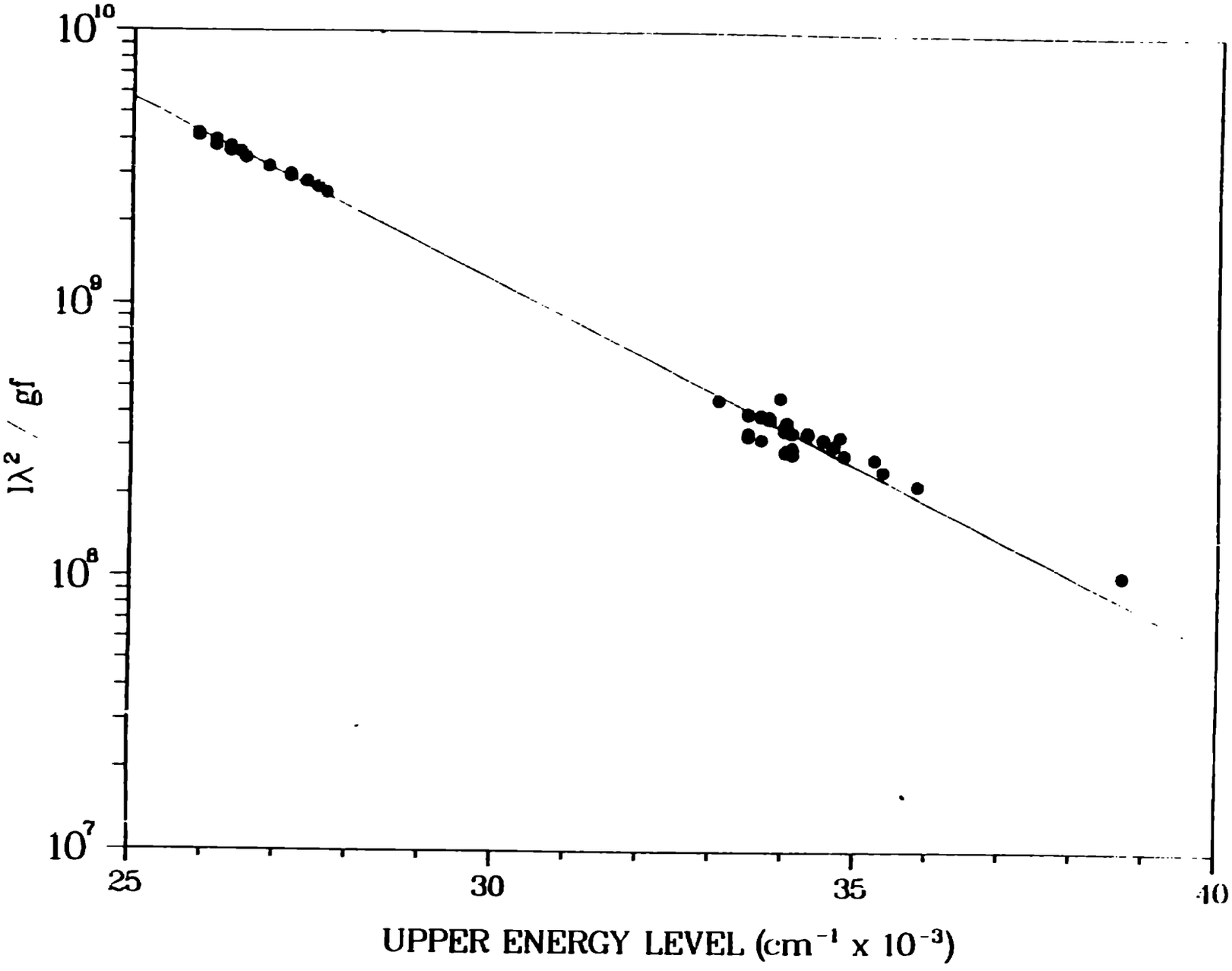
10^{10}
10^{9}
10^{8}
10^{7}
$I\lambda^2 / gf$
25
30
35
40
UPPER ENERGY LEVEL (cm^{-1} x 10^{-3})

Figure 7

KITT PEAK FOURIER TRANSFORM SPECTROMETER

Spectral Range Capability	250 nm – 16 μm
Spectral Range Observed	290 – 390 nm
Maximum Optical Path Difference Capability	1 meter
Maximum Optical Path Difference Utilized	7.06 cm
Resolution Capability	.005 cm^{-1}
Resolution Utilized	.071 cm^{-1}
Aperture Diameter	10 mm
Beamsplitter Utilized	Ultrasil fused silica (Al coating)
Detector Utilized	silicon photodiode (blue enhanced)
Detector Filters	$CuSO_4$ and Corning 7–54
Interferogram Size	10^6 POINTS
Interferograms Co–added	24

Table 1

ICP OPERATING CONDITIONS

source unit	Plasma Therm 2500 series
frequency	27.12 MHz
power	1.1 kwatt
coolant flow	12.5 LPM
auxiliary flow	for ignition only
nebulizer flow	1.0 LPM
nebulizer back pressure	16 psi
nebulizer	fritted disc Los Alamos design
viewing height	11 mm
laboratory atmosphere	601 torr

Table 2

TEST DATA

DEFINED					DETERMINED			
S/N	INT	$\Delta\sigma$ (cm^{-1})	$\Delta\sigma_G$ (cm^{-1})	$\Delta\sigma_L$ (cm^{-1})	% RSD INT	% RSD $\Delta\sigma$	% RSD [illegible]	% RSD $\Delta\sigma_L$
10	0.10	.220	.20546	.0246	8.88	8.23	27.36	126.16
100	1.00	.220	.20546	.0246	0.82	1.00	3.39	35.94
1000	10.00	.220	.20546	.0246	0.08	0.10	0.34	3.76

Table 3

TEST DATA

DEFINED		DETERMINED				
S/N	$\Delta\sigma_G$ (cm^{-1})	Mean $\Delta\sigma_G$ (cm^{-1})	%RSD $\Delta\sigma_G$	Mean $\frac{\Delta\sigma_G}{\sigma} \times 10^6$	Mean T_D(K)	% RSD T_D
10	.20546	.18854	27.36	7.25	5726	41.93
100	.20546	.20481	3.39	7.71	6483	6.74
1000	.20546	.20548	0.34	7.74	6525	0.77

Table 4

TABLE 5

σ	λ	S/N	$\Delta\sigma$	$\Delta\lambda$	$\Delta\sigma_G$	$\Delta\sigma_L$	$\frac{a}{}$	$\frac{\Delta\sigma_G}{\sigma}\times 10^6$	T_D
24709.949	404.5810	144	.208	.00341	.191	.031	.14	7.72	6509
25436.195	393.0293	215	.204	.00315	.196	.016	.07	7.70	6469
25451.588	392.7916	198	.205	.00316	.191	.026	.11	7.49	6135
25484.076	392.2908	177	.205	.00316	.190	.027	.12	7.46	6056
25501.328	392.2540	125	.205	.00315	.190	.027	.12	7.45	6048
25635.713	389.9703	252	.207	.00315	.194	.023	.10	7.57	6239
25662.371	389.5652	177	.209	.00317	.196	.024	.10	7.62	6355
25724.268	388.6278	830	.206	.00311	.193	.024	.10	7.51	6132
25775.396	387.8569	385	.206	.00310	.198	.019	.08	7.69	6429
25779.076	387.8015	126	.217	.00326	.198	.034	.14	7.68	6427
25815.803	387.2498	124	.211	.00317	.193	.033	.14	7.48	6089
25862.404	386.5520	106	.218	.00326	.193	.044	.19	7.48	6067
25900.012	385.9908	2380	.209	.00311	.195	.025	.11	7.54	6175
25923.785	385.6368	573	.208	.00309	.196	.022	.09	7.57	6227
25966.904	384.9964	140	.215	.00319	.206	.017	.07	7.93	6856
26027.193	384.1046	265	.221	.00326	.200	.037	.15	7.70	6433
26031.334	384.0435	346	.214	.00316	.197	.032	.14	7.56	6259
26073.529	383.4220	632	.215	.00316	.200	.027	.11	7.70	6410
26117.117	382.7820	406	.222	.00325	.200	.039	.16	7.66	6389
26130.373	382.5878	1253	.217	.00318	.202	.027	.11	7.73	6510
26140.201	382.4440	595	.210	.00307	.196	.026	.11	7.48	6125
26167.688	382.0423	2036	.217	.00317	.203	.027	.11	7.74	6556
26199.129	381.5838	692	.222	.00323	.198	.042	.18	7.58	6222
26218.893	381.2961	140	.213	.00310	.190	.041	.18	7.25	5721
26311.473	379.9545	197	.217	.00313	.197	.035	.15	7.50	6107
26318.648	379.8508	113	.220	.00318	.199	.037	.15	7.57	6228
26342.984	379.4999	225	.216	.00311	.196	.037	.16	7.45	6031
26392.516	378.7877	171	.219	.00314	.204	.027	.11	7.73	6509
26537.451	376.7189	504	.220	.00312	.203	.032	.13	7.64	6375
26561.443	376.3786	759	.219	.00310	.202	.030	.12	7.61	6301
26600.711	375.8230	1313	.219	.00309	.203	.029	.12	7.64	6345
26662.768	374.9482	2220	.220	.00309	.203	.030	.12	7.63	6315
26671.475	374.8258	1084	.215	.00302	.201	.026	.11	7.53	6187
26688.297	374.5896	500	.215	.00302	.201	.026	.11	7.51	6179
26690.709	374.5557	2000	.215	.00302	.201	.025	.10	7.54	6178
26706.381	374.3359	215	.222	.00311	.206	.029	.12	7.70	6482
26750.910	373.7128	3346	.215	.00300	.202	.025	.10	7.54	6212
26767.145	373.4861	3541	.222	.00310	.205	.031	.13	7.65	6390
26778.238	373.3314	445	.216	.00301	.201	.028	.12	7.50	6138
26819.168	372.7616	330	.221	.00307	.202	.033	.14	7.55	6180
26855.600	372.2559	609	.215	.00298	.201	.027	.11	7.47	6103
26874.572	371.9931	5227	.217	.00300	.203	.026	.11	7.55	6216
26952.006	370.9243	350	.223	.00307	.206	.030	.12	7.66	6364
26978.781	370.5562	593	.217	.00298	.203	.025	.10	7.52	6168
27111.266	368.7454	254	.223	.00303	.208	.028	.11	7.68	6412
27166.844	367.9910	355	.223	.00302	.204	.026	.11	7.51	6143
27405.674	364.7840	1033	.228	.00303	.210	.032	.13	7.66	6397
27529.283	363.1460	1261	.228	.00301	.211	.032	.13	7.65	6400
27625.857	361.8765	1157	.228	.00299	.211	.032	.13	7.63	6355

27701.707	360.8856	893	.230	.00300	.213	.032	.13	7.67	6441
27718.449	360.6676	117	.229	.00298	.208	.038	.15	7.51	6135
27870.637	358.6982	176	.229	.00295	.209	.037	.15	7.49	6126
27883.584	358.5316	187	.231	.00297	.210	.038	.15	7.52	6179
27915.705	358.1190	3804	.232	.00298	.214	.032	.12	7.68	6402
28001.223	357.0253	164	.260	.00332	.208	.088	.35	7.44	6011
28002.463	357.0095	1871	.233	.00297	.215	.031	.12	7.69	6422
28039.523	356.5376	806	.232	.00295	.215	.031	.12	7.66	6405
28093.605	355.8512	233	.232	.00294	.213	.035	.14	7.58	6262
28121.965	355.4924	121	.264	.00334	.214	.088	.34	7.59	6309
28352.340	352.6038	124	.226	.00281	.209	.032	.13	7.36	5920
28390.818	352.1258	111	.236	.00293	.211	.044	.17	7.44	6017
28580.916	349.7837	201	.231	.00283	.212	.035	.14	7.40	5994
28640.414	349.0571	648	.231	.00282	.215	.029	.11	7.50	6139
28754.686	347.6698	213	.233	.00282	.218	.026	.10	7.60	6262
28765.043	347.5447	651	.232	.00280	.217	.029	.11	7.53	6200
28844.629	346.5857	439	.233	.00280	.218	.027	.10	7.57	6223
29028.754	344.3873	288	.234	.00278	.219	.028	.11	7.54	6201
29053.115	344.0985	799	.235	.00278	.220	.027	.10	7.58	6247
29056.348	344.0602	1741	.235	.00278	.220	.027	.10	7.56	6245
32680.031	305.9083	230	.269	.00252	.256	.025	.08	7.82	6685
32803.141	304.7602	273	.270	.00251	.259	.020	.06	7.89	6792
32913.465	303.7386	200	.269	.00248	.257	.022	.07	7.81	6642
33039.051	302.5840	114	.270	.00247	.255	.026	.08	7.73	6490
33091.211	302.1070	396	.272	.00248	.258	.026	.08	7.78	6622
33097.590	302.0488	115	.268	.00245	.261	.013	.04	7.89	6775
33233.492	300.8136	110	.274	.00248	.261	.025	.08	7.84	6719
33313.121	300.0945	200	.272	.00245	.253	.034	.11	7.60	6284
33385.664	299.4424	228	.272	.00244	.255	.030	.10	7.64	6356
33507.145	298.3567	211	.276	.00246	.263	.024	.08	7.84	6712
33623.609	297.3233	151	.277	.00245	.261	.028	.09	7.77	6564
33695.422	296.6896	291	.279	.00246	.266	.024	.08	7.89	6789

IRON I EXCITATION TEMPERATURE

gf reference	excitation temperature	estimated error	number of lines
BLACKWELL et al.	4732	62	51
BRIDGES and KORNBLITH	4695	69	61
HUBER and PARKINSON	4825	85	31

Table 6